Excited-State Interactions for $[Au(CN)_2^-]_n$ and $[Ag(CN)_2^-]_n$ Oligomers in Solution. Formation of Luminescent Gold−Gold Bonded Excimers and Exciplexes

Manal A. Rawashdeh-Omary,[†,‡] Mohammad A. Omary,[‡,§] Howard H. Patterson,*[,†] and John P. Fackler, Jr.*[,‡]

Contribution from the Department of Chemistry, University of Maine, Orono, Maine 04469, and the Department of Chemistry, Texas A&M University, College Station, Texas 77843

Received May 11, 2001. Revised Manuscript Received August 24, 2001

Abstract: Solutions of $K[Au(CN)_2]$ and $K[Ag(CN)_2]$ in water and methanol exhibit strong photoluminescence. Aqueous solutions of $K[Au(CN)_2]$ at ambient temperature exhibit luminescence at concentration levels of $\geq 10^{-2}$ M, while frozen methanol glasses (77 K) exhibit strong luminescence with concentrations as low as 10^{-5} M. The corresponding concentration limits for $K[Ag(CN)_2]$ solutions are 10^{-1} M at ambient temperature and 10^{-4} M at 77 K. Systematic variations in concentration, solvent, temperature, and excitation wavelength tune the luminescence energy of both $K[Au(CN)_2]$ and $K[Ag(CN)_2]$ solutions by $>15 \times 10^3$ cm^{-1} in the UV−visible region. The luminescence bands have been individually assigned to $*[Au(CN)_2^-]_n$ and $*[Ag(CN)_2^-]_n$ excimers and exciplexes that differ in "*n*" and geometry. The luminescence of Au(I) compounds is related for the first time to Au−Au bonded excimers and exciplexes similar to those reported earlier for Ag(I) compounds. Fully optimized unrestricted open-shell MP2 calculations for the lowest-energy triplet excited state of staggered $[Au(CN)_2^-]_2$ show the formation of a Au−Au σ single bond (2.66 Å) in the triplet excimer, compared to a weaker ground-state aurophilic bond (2.96 Å). The corresponding frequency calculations revealed Au−Au Raman-active stretching frequencies at 89.8 and 165.7 cm^{-1} associated with the ground state and lowest triplet excited state, respectively. The experimental evidence of the exciplex assignment includes the extremely large Stokes shifts and the structureless feature of the luminescence bands, which suggest very distorted excited states. Extended Hückel (EH) calculations for $[M(CN)_2^-]_n$ and $*[M(CN)_2^-]_n$ models (M = Au, Ag; $n = 2, 3$) indicate the formation of M−M bonds in the first excited electronic states. From the average EH values for staggered dimers and trimers, the excited-state Au−Au and Ag−Ag bond energies are predicted to be 104 and 112 kJ/mol, respectively. The corresponding bond energies in the ground state are 32 and 25 kJ/mol, respectively.

Introduction

The past three decades have witnessed continuing interest in the photophysics and photochemistry of d^{10} complexes of the coinage metal monovalent cations, as attested by the large number of reviews about this topic.[1−7] The electronic spectra and structure of these systems clearly relate to the presence of closed-shell metal−metal bonding,[8,9] exciplex formation,[10] electron transfer,[11] energy transfer,[12−14] and chemical reactivity.[15] Moreover, a number of applications for use of materials based on d^{10} coinage metal ions have been linked to their electronic structure. For example, it has been suggested that the therapeutic action of gold drugs for rheumatoid arthritis[16] is related to the ability of Au(I) compounds to quench the singlet oxygen $^1\Delta_g$ state at 7752 cm^{-1}.[17] The existing and/or potential uses based on Cu(I) materials as photosensitizers for water splitting,[18] tunable solid-state lasers,[19] and photocatalysts;[20] Au(I) materials as biosensors,[21] photocatalysts,[22] optical sensors,[23] and new types of liquid crystal phases;[24] and Ag(I)

[†] University of Maine.
[‡] Texas A&M University.
[§] Permanent Address: Department of Chemistry, University of North Texas, Denton, TX 76203.

(1) Kutal, C. *Coord. Chem. Rev.* **1990**, *99*, 213.
(2) Horváth, O. *Coord. Chem. Rev.* **1994**, *135/136*, 303.
(3) Jansen, M. *Angew. Chem., Int. Ed. Engl.* **1987**, *26*, 1098.
(4) Ford, P. C.; Vogler, A. *Acc. Chem. Res.* **1993**, *26*, 220.
(5) Forward, J. M.; Fackler, J. P., Jr.; Assefa, Z. Photophysical and Photochemical Properties of Gold(I) Complexes. In *Optoelectronic Properties of Inorganic Compounds*; Roundhill, D. M.; Fackler, J. P., Jr., Eds.; Plenum Press: New York, 1999; Chapter 6.
(6) Bowmaker, G. A. Spectroscopic Methods in Gold Chemistry. In *Gold: Progress in Chemistry, Biochemistry and Technology*; Schmidbaur, H., Ed.; Wiley: Chichester, New York, 1999, Chapter 21.
(7) Patterson, H. H.; Kanan, S. M.; Omary, M. A. *Coord. Chem. Rev.* **2000**, *208*, 227.
(8) Pyykkö, P. *Chem. Rev.* **1997**, *97*, 599.
(9) Schmidbaur, H. *Chem. Soc. Rev.* **1995**, 391.
(10) Omary, M. A.; Patterson, H. H. *J. Am. Chem. Soc.* **1998**, *120*, 7696.
(11) (a) Li, D.; Che, C. M.; Kwong, H. L.; Yam, V. W. W. *J. Chem. Soc., Dalton Trans.* **1992**, 3325. (b) Che, C. M.; Kwong, H. L.; Poon, C. K.; Yam, V. W. W. *J. Chem. Soc., Dalton Trans.* **1990**, 3215.
(12) Rawashdeh-Omary, M. A.; Larochelle, C. L.; Patterson, H. H. *Inorg. Chem.* **2000**, *39*, 4527.
(13) (a) Assefa, Z.; Shankle, G.; Patterson, H. H.; Reynolds, R. *Inorg. Chem.* **1994**, *33*, 2187. (b) Assefa, Z.; Patterson, H. H. *Inorg. Chem.* **1994**, *33*, 6195.
(14) Yersin, H.; Trümbach, D.; Strasser, J.; Patterson, H. H.; Assefa, Z. *Inorg. Chem.* **1998**, *37*, 3209.
(15) Low, J. J.; Goddard, W. A., III. *J. Am. Chem. Soc.* **1986**, *108*, 6115.
(16) Shaw, C. F., III. The Biochemistry of Gold. In *Gold: Progress in Chemistry, Biochemistry and Technology*; Schmidbaur, H., Ed.; Wiley: Chichester, New York, 1999, Chapter 10.
(17) Corey, E. J.; Mahrotra, M. M.; Khan, A. U. *Science* **1987**, *236*, 68.
(18) Edel, A.; Marnot, P. A.; Sauvage, J. P. *Nouv. J. Chim.* **1984**, *8*, 495.
(19) (a) Kruglik, G. S.; Skripko, G. A.; Shkadarevich, A. P.; Ermolenko, N. N.; Gorodetskaya, O. G.; Belokon, M. V.; Shagov, A. A.; Zolotareva, L. E. *Opt. Spectrosk.* **1985**, *59*, 439. (b) Moine, B.; Pedrini, C.; Duloisy, E.; Boutinaud, P.; Parent, C.; Le Flem, G. *J. Phys. IV* **1991**, *C7*, 289.

10.1021/ja011176j CCC: $20.00
Published on Web 10/23/2001

materials as photographic materials,[25] optical fibers,[26] photocatalysts for NO decomposition,[27] semiconductors and photoconductors[3,28] are all strongly related to the electronic structure and excited-state properties. The ability to tune the excited-state properties is essential in order to use the luminescent materials in potential applications. The observation of photoluminescence in aqueous solutions is of special importance, because this may allow for monitoring and probing biological processes associated with the luminescent material. For example, a variety of Au(I) complexes with ligands such as cyanides and pseudohalides have been proposed for the treatment of retroviral diseases such as AIDS in an infected host.[29] Gold(I) complexes that are luminescent in aqueous solutions are scarce, with the first example reported by Fackler and co-workers in 1995.[30] In the present study, we report strong, tunable photoluminescence from aqueous solutions of dicyanoaurate(I), one of the biologically relevant complexes mentioned above.

The dicyanoaurates(I) and dicyanoargentates(I) continue to attract our attention because of their fascinating spectroscopic properties. These stable complexes have been known for a very long time but have continued to receive interest because of their important scientific[31−33] and industrial applications in fields such as semiconductors,[34] medicine,[16,29] and gold extraction.[35] The latter application involves adsorption of the dicyanoaurates(I) via the carbon-in-pulp (CIP) process, in which the oligomerization of $Au(CN)_2^-$ ions is now understood to play an important role.[35] The complexes $Au(CN)_2^-$ and $Ag(CN)_2^-$ are ideal systems to study $d^{10}-d^{10}$ closed-shell interactions because of the absence of ligand assistance, which often obscures the extent of these interactions. The reasonable stability of these compounds to air, moisture, temperature, and light, as well as their solubility in water, are also important practical advantages. In a recent study, some of us have characterized the oligomerization processes for $Au(CN)_2^-$ and $Ag(CN)_2^-$ ions in solution and presented a comparison of Au−Au bonding and Ag−Ag bonding in the ground state.[33] Increasing the concentration leads to the appearance of distinct absorption bands at much lower energies than are found for the monomer absorption band energies in dilute solutions. The new low-energy bands in concentrated solutions have been assigned to various oligomers, for which the formation constants and free energies have been calculated. Here, we report excited-state interactions of the dicyanoaurates(I) and dicyanoargentates(I) in solution. Earlier work has demonstrated the presence of significant excited-state interactions in solid-state systems of $Ag(CN)_2^-$, which lead to the formation of luminescent Ag−Ag bonded excimers and exciplexes with the formula $*[Ag(CN)_2^-]_n$ ($n \geq 2$).[10,36] The consequence of exciplex formation on the excited-state properties of $Ag(CN)_2^-$ solids is illustrated by the optical phenomenon, "exciplex tuning", which entails the tuning of the luminescence spectra to distinct bands characteristic of $*[Ag(CN)_2^-]_n$ exciplexes. Remarkably, the excited-state energies have been tuned by more than 18 000 cm^{-1} in the UV and visible regions *in one single crystal* of $Ag(CN)_2^-$/KCl by site-selective excitation of individual oligomers.[10] The relative intensities of the exciplex bands can be controlled by varying the dopant concentration,[37] temperature (luminescence thermochromism),[38] alkali halide host,[38] and controlled irradiation.[39] Examples illustrating the importance of these findings in scientific and practical applications have been reported in two recent publications by some of us about tunable energy transfer to lanthanide ions[12] and the photocatalytic action of Ag(I)-doped ZSM-5 zeolites in the decomposition of nitric oxide.[27]

A major objective of the present investigation is to study whether exciplex behavior exists for $[Au(CN)_2^-]_n$ oligomer ions, similar to the situation reported earlier for $[Ag(CN)_2^-]_n$ species. The concept of excited-state interactions that lead to metal−metal bond formation is emphasized on the basis of experimental and theoretical evidence. Also, we present comparisons between excited-state interactions versus ground-state interactions for both $[Au(CN)_2^-]_n$ and $[Ag(CN)_2^-]_n$.

Experimental Section

Solutions of $K[Ag(CN)_2]$ and $K[Au(CN)_2]$ were prepared by directly dissolving the solids (≥99.9% pure) in doubly distilled water and reagent-grade methanol. The solid compounds were obtained from Alfa Aesar and stored in desiccators in the dark until used. Steady-state photoluminescence spectra were recorded with a Model QuantaMaster-1046 photoluminescence spectrophotometer from Photon Technology International, PTI. The instrument is equipped with two excitation monochromators and a 75 W xenon lamp. Luminescence measurements at ambient temperatures were carried out for aqueous and methanolic solutions of $K[Ag(CN)_2]$ and $K[Au(CN)_2]$ in standard 1-cm quartz cuvettes. Low-temperature luminescence measurements were carried out using frozen solutions of $K[Ag(CN)_2]$ and $K[Au(CN)_2]$ in water and methanol. The solutions were placed in supracell quartz capillary tubes and inserted into a liquid nitrogen Dewar flask with a supracell quartz window. Measurements for pure solvents were carried out as a control.

(20) (a) Anpo, M.; Matsuoka, M.; Yamashita, H. *Catal. Today* **1997**, *35*, 177. (b) Anpo, M.; Zhang, S.; Mishma, H.; Matsuoka, M.; Yamashita, H. *Catal. Today* **1997**, *39*, 159.

(21) Blonder, R.; Levi, S.; Tao, G.; Ben-Dov, I.; Willner, I. *J. Am. Chem. Soc.* **1997**, *119*, 10467.

(22) Wolf, M. O.; Fox, M. A. *J. Am. Chem. Soc.* **1995**, *117*, 1845.

(23) Mansour, M. A.; Connick, W. B.; Lachicotte, R. J.; Gysling, H. J.; Eisenberg, R. *J. Am. Chem. Soc.* **1998**, *120*, 1329.

(24) (a) Kaharu, T.; Ishii, R.; Takahashi, S. *J. Chem. Soc., Chem. Commun.* **1994**, 1349. (b) Bachman, R. E.; Fioritto, M. S.; Fetics, S. K.; Cocker, T. M. *J. Am. Chem. Soc.* **2001**, *123*, 5376.

(25) (a) Von der Austin, W.; Stolz, H. *J. Phys. Chem. Solids* **1990**, *51*, 765. (b) Hamilton, J. F. *Adv. Phys.* **1988**, *37*, 359. (c) Ueta, M.; Kanzaki, H.; Kabayashi, K.; Toyozawa, Y.; Hanamura, E. *Excitonic Processes in Solids*; Springer: Berlin, 1986; pp 309−69.

(26) (a) Moser, F.; Barkay, N.; Levite, A.; Margalit, E.; Paiss, I.; Sa'ar, A.; Schnitzer, I.; Zur, A.; Katzir, A. *Proc. SPIE-Int. Soc. Opt. Eng.* **1990**, *1228*, 128. (b) Baetzold, R. C. *J. Phys. Chem. B* **1997**, *101*, 8180.

(27) Kanan, S. M.; Omary, M. A.; Patterson, H. H.; Matsuoka, M.; Anpo, M. *J. Phys. Chem. B.* **2000**, *104*, 3507.

(28) (a) Köhler, B. U.; Weppner, W.; Jansen, M. *J. Solid State Chem.* **1985**, *57*, 227. (b) Gruber, H.; Hess, H.; Popitsch, A.; Fischer, A. P. *J. Electrochem. Soc.* **1982**, *129*, 369. (c) Popitsch, A. *J. Crystallogr. Spectrosc. Res.* **1985**, *15*, 603.

(29) Elder, R. C.; Elder, K. T. U.S. Patent 5603963, 1997.

(30) (a) Forward, J. M.; Assefa, Z.; Fackler, J. P., Jr. *J. Am. Chem. Soc.* **1995**, *117*, 9103. (b) For a summary, see: Fackler, J. P., Jr.; Grant, T. A. *Chemist (Washington, D.C.)* **1998**, *75*, 29.

(31) Sharpe, A. G. *The Chemistry of Cyano Complexes of the Transition Metals*; Academic Press: London, 1976.

(32) (a) Mason, W. R. *J. Am. Chem. Soc.* **1973**, *95*, 3573. (b) Mason, W. R. *J. Am. Chem. Soc.* **1976**, *98*, 5182.

(33) Rawashdeh-Omary, M. A.; Omary, M. A.; Patterson, H. H. *J. Am. Chem. Soc.* **2000**, *122*, 10371.

(34) (a) Kurmoo, M.; Day, P.; Mitani, T.; Kitagawa, H.; Shimoda, H.; Yoshida, D.; Guionneau, P.; Barrans, Y.; Chasseau, D.; Ducasse, L. *Bull. Chem. Soc. Jpn.* **1996**, *69*, 1233. (b) Chasseau, D.; Guionneau, P.; Rahal, M.; Bravic, G.; Gaultier, J.; Ducasse, L.; Kurmoo, M.; Day, P. *Synth. Met.* **1995**, *70*, 945. (c) Fujiwara, H.; Kobayashi, H. *Chem. Commun.* **1999**, *23*, 2417. (d) Kurmoo, M.; Pritchard, K. L.; Talham, D. R.; Day, P.; Stringer, A. M.; Howard, J. A. K. *Acta Crystallogr.* **1990**, *B46*, 348.

(35) Adams, M. D.; Johns, M. W.; Dew, D. W. Recovery of Gold from Ores and Environmental Aspects. In *Gold: Progress in Chemistry, Biochemistry and Technology*; Schmidbaur, H., Ed.; Wiley: Chichester, New York, 1999; Chapter 3.

(36) Omary, M. A.; Patterson, H. H. *Inorg. Chem.* **1998**, *37*, 1060.

(37) Omary, M. A.; Hall, D. R.; Shankle, G. E.; Siemiarczuck, A.; Patterson, H. H. *J. Phys. Chem. B.* **1999**, *103*, 3845.

(38) Rawashdeh-Omary, M. A.; Omary, M. A.; Shankle, G. E.; Patterson, H. H. *J. Phys. Chem. B.* **2000**, 104, 6143.

(39) Srisook, N. M.S. Thesis, Graduate School, University of Maine, 2000.

Chart 1. Geometries of the Various Molecular Models of $[M(CN)_2^-]_n$ (M = Au, Ag; n = 2, 3) Used in the Computations

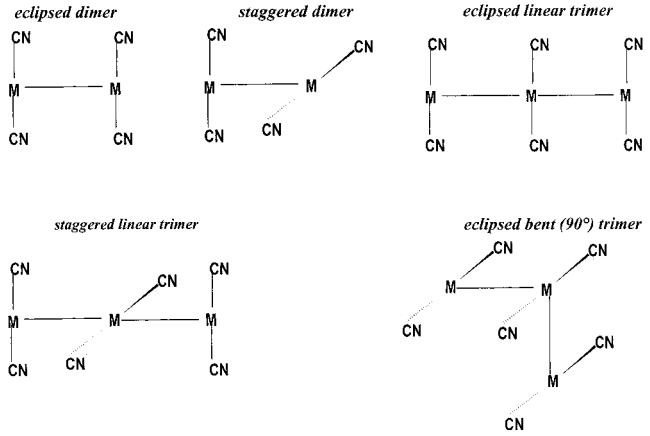

Computational Details

Chart 1 shows the geometries of the various molecular models used in the computations. Calculations at the Møller−Plesset 2nd order Perturbation (MP2)[40] level of theory were performed for staggered $[Au(CN)_2^-]_2$ using the Gaussian 98 suite of programs.[41] Full geometry optimizations were carried out for the ground state at the MP2 level and for the first triplet excited state using the unrestricted open-shell MP2 method (UMP2).[40] A Huzinaga/Dunning basis set of a double-ζ quality[42] with a polarization function (D95*) was used for carbon and nitrogen atoms. A small-core effective core potential (ECP) developed by Hay and Wadt[43] was used for gold atoms to represent the 60 core electrons ($1s^2\ 2s^2\ 2p^6$... $4d^{10}\ 4f^{14}$). The Hay and Wadt double-ζ basis set was modified as described by Couty and Hall[44] to include parameters for the outer 6p functions with a 341/541/21 split for the $5s^25p^65d^{10}6s^1$ valence electrons. The ECP for gold incorporates two relativistic effects for the core electrons, mass velocity and Darwin, and thus represents the dominant relativistic contributions to the behavior of the outer electrons. Extended Hückel (EH) calculations were carried out using the FORTICON8 program (QCMP011) with relativistic parameters.[45] The details of the EH calculation, including the parameters and interatomic distances used were published elsewhere.[33,37]

Results and Discussion

1. Luminescence of K[Au(CN)$_2$] Solutions. Figure 1 shows the emission spectra of $K[Au(CN)_2]$ aqueous solutions versus concentration at ambient temperature (~20 °C). Two major emission bands appear at all concentrations, a higher-energy (HE) band and a lower-energy (LE) band with maxima near 400−410 and 430−470 nm, respectively. Two general trends are observed as the $Au(CN)_2^-$ concentration increases: an increase in the relative intensity of the LE/HE bands and a red shift in the energy of the LE band. The position of the HE band remains virtually unaffected with concentration. The HE and LE bands have virtually the same excitation spectra. For example, both the 0.200 and 0.623 M solutions show the same excitation profile when the emission is monitored at wavelengths that correspond to the LE band and to the HE band. This result suggests the presence of energy transfer from the exciton characteristic of the HE band to the exciton characteristic of the LE band.

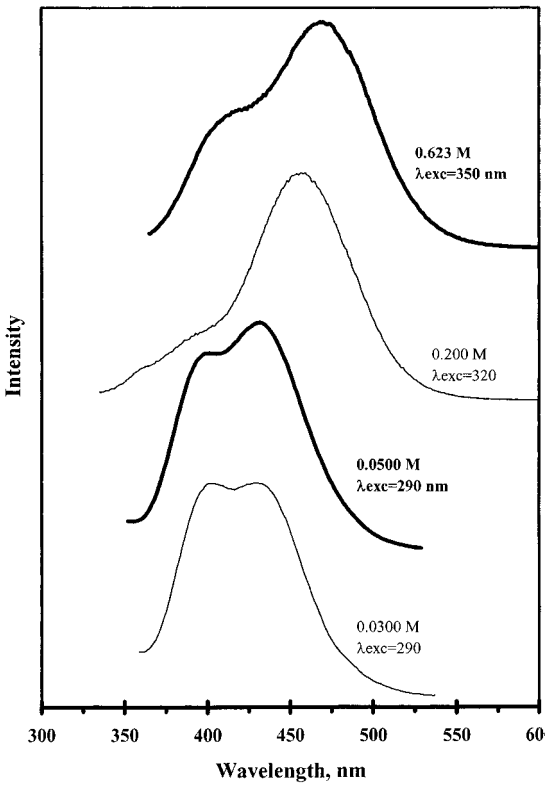

Figure 1. Emission spectra versus concentration of $K[Au(CN)_2]$ in aqueous solutions at ambient temperature. The excitation wavelengths correspond to the peaks in the excitation spectra for each solution.

We assign the HE and LE bands to $*[Au(CN)_2^-]_{n_1}$ and $*[Au(CN)_2^-]_{n_2}$ with $n_2 > n_1$. Upon increasing the total $K[Au(CN)_2]$ concentration, the statistical distribution of the larger oligomer increases, leading to higher populations of the $*[Au(CN)_2^-]_{n_2}$ excitons and, hence, a stronger LE emission. We attribute the red shift of the LE band to the formation of larger oligomers. A similar observation and explanation were reported for the tetracyanoplatinates(II).[46,47] To rule out the possibility that the red shift of the LE band in Figure 1 could be related to a change in the electrostatic environment around the dicyanoaurate(I) anions, we have carried out a similar experiment in which the total $K[Au(CN)_2]$ concentration was varied while holding the ionic strength constant. Both the emission and excitation energies showed a red shift upon increasing the total $K[Au(CN)_2]$ concentration in 0.8 M KCl deaerated aqueous solutions. A plot of the emission energy (cm^{-1}) versus molar concentration shows a quadratic relationship ($y = 38\,467x^2 - 15\,917x + 23\,479$) with a squared correlation coefficient of unity

(40) (a) Pople, J. A.; Binkley, J. S.; Seeger, R. *Int. J. Quantum Chem. Symp.* **1976**, *10*, 1. (b) Moller, C.; Plesset, M. S. *Phys. Rev.* **1934**, *46*, 618. (c) Tozer, D. J.; Andrews, J. S.; Amos, R. D.; Handy, N. C. *Chem. Phys. Lett.* **1992**, *199*, 229. (d) Carsky, P.; Hubak, E. *Theoe. Chim. Acta* **1991**, *80*, 407. (e) Osamura, Y.; Yamaguchi, Y.; Henry, I.; Schaefer, F. *Chem. Phys.* **1986**, *103*, 227.

(41) Frisch, M. J.; Trucks, G. W.; Schlegel, H. B.; Scuseria, G. E.; Robb, M. A.; Cheeseman, J. R.; Zakrzewski, V. G.; Montgomery, J. A., Jr.; Stratmann, R. E.; Burant, J. C.; Dapprich, S.; Millam, J. M.; Daniels, A. D.; Kudin, K. N.; Strain, M. C.; Farkas, O.; Tomasi, J.; Barone, V.; Cossi, M.; Cammi, R.; Mennucci, B.; Pomelli, C.; Adamo, C.; Clifford, S.; Ochterski, J.; Petersson, G. A.; Ayala, P. Y.; Cui, Q.; Morokuma, K.; Malick, D. K.; Rabuck, A. D.; Raghavachari, K.; Foresman, J. B.; Cioslowski, J.; Ortiz, J. V.; Stefanov, B. B.; Liu, G.; Liashenko, A.; Piskorz, P.; Komaromi, I.; Gomperts, R.; Martin, R. L.; Fox, D. J.; Keith, T.; Al-Laham, M. A.; Peng, C. Y.; Nanayakkara, A.; Gonzalez, C.; Challacombe, M.; Gill, P. M. W.; Johnson, B. G.; Chen, W.; Wong, M. W.; Andres, J. L.; Head-Gordon, M.; Replogle, E. S.; Pople, J. A. *Gaussian 98*, revision A.6; Gaussian, Inc.: Pittsburgh, PA, 1998.

(42) Dunning, T. H., Jr.; Hay, P. J. In *Modern Theoretical Chemistry*, Schaefer, H. F., III, Ed.; Plenum: New York, 1976; Vol. 3, p 1.

(43) Hay, P. J.; Wadt, W. R. *J. Chem. Phys.* **1985**, *82*, 270.

(44) Couty, M.; Hall, M. B. *J. Comput. Chem.* **1996**, *17*, 1359.

(45) Pyykkö, P.; Lohr, L. L. *Inorg. Chem.* **1981**, *20*, 1950.

(46) Schindler, J. W.; Fukuda, R. C.; Adamson, A. W. *J. Am. Chem. Soc.* **1982**, *104*, 3596.

(47) Gliemann, G.; Lechner, A. *J. Am. Chem. Soc.* **1989**, *111*, 7469.

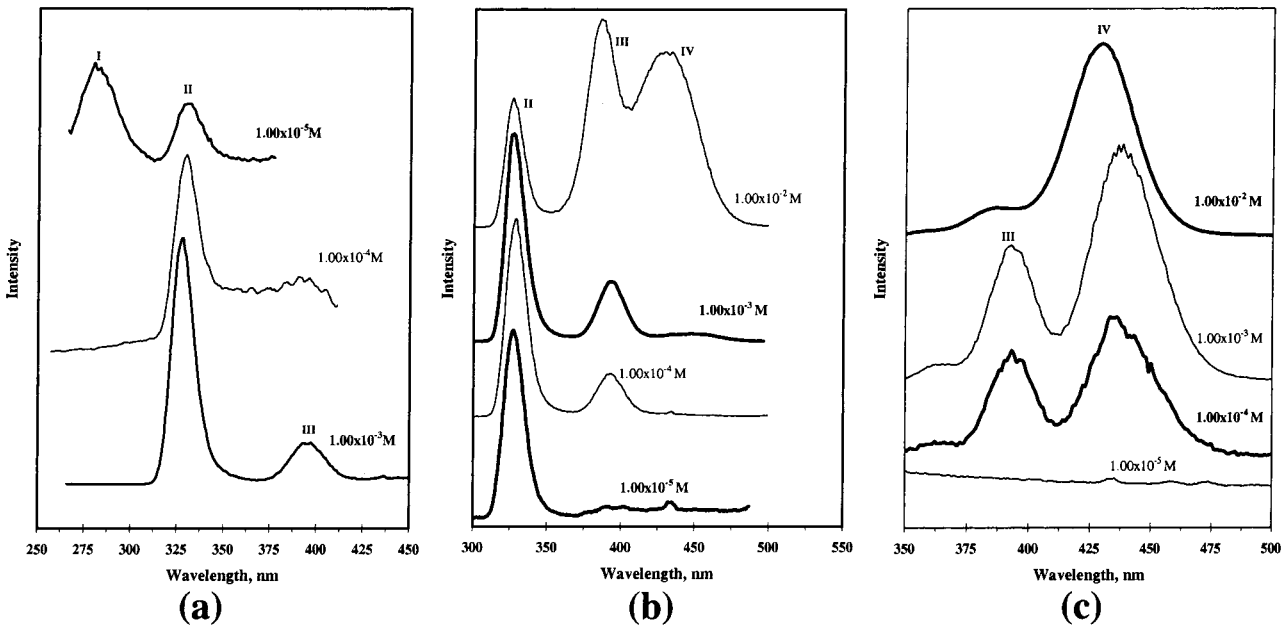

Figure 2. Emission spectra versus concentration of $K[Au(CN)_2]$ in methanol frozen solutions (77 K). The excitation wavelengths are selected at 245 nm (a), 260 nm (b), and 315 nm (c) to show emission of oligomers with different sizes.

($R^2 = 1$). The corresponding equation for the excitation energy was $y = 49\,002x^2 - 33\,330x + 35\,101$; $R^2 = 1$. The growth of the oligomer with a quadratic relationship is consistent with the 2-dimensional layered structure observed in the crystal structures of the dicyanoaurates(I).[48] As the solution concentration of $K[Au(CN)_2]$ increases toward saturation, the solid-state structure is approached, and hence, the diffusion of $Au(CN)_2^-$ ions should follow a quadratic equation as opposed to a linear equation. The emission energy for the nearly saturated solution approached but remained higher than the emission energy of solid $KAu(CN)_2$.[48]

While aqueous solutions of $K[Au(CN)_2]$ at ambient temperature show luminescence at concentrations levels of $\geq 10^{-2}$ M, frozen solutions in methanol glasses exhibit strong luminescence with concentrations as low as 10^{-5} M. The excitation spectra of $K[Au(CN)_2]$ solutions in methanol at 77 K show peaks at much longer wavelengths than the absorption peaks of the same solutions at ambient temperature,[33] which indicates the oligomerization of $Au(CN)_2^-$ species even at concentrations as low as 10^{-5} M. Emission spectra have been obtained using excitation wavelengths that correspond to the excitation bands (the excitation spectra have been reported in ref 33). Figure 2a shows the emission spectra versus concentration using wavelengths that correspond to the highest-energy excitation band (240−250 nm). Figure 2a shows that the 10^{-3} M and 10^{-4} M solutions exhibit emission bands near 325 and 393 nm with a stronger intensity for the 325 nm band. As the concentration is decreased to 10^{-5} M, a new high-energy band appears with an emission maximum of 280 nm. A further decimal dilution has not resulted in detectable luminescence for the $K[Au(CN)_2]$ frozen solutions in methanol. Therefore, the 280 nm emission band (labeled I) for the 10^{-5} M solution represents the highest-energy limit for the $Au(CN)_2^-$ luminescence and, therefore, should be assigned to the "smallest" $[Au(CN)_2^-]_n$ oligomer, while the lower-energy bands labeled II and III correspond to "larger" oligomers. Figure 2b shows the emission spectra versus concentration using 260 nm excitation. The major emission of the 10^{-5} M solution changes from band I to band II as the excitation wavelength is changed from 240 to 260 nm. Figure 2b also shows that a progressive increase in concentration to 10^{-4}, 10^{-3}, and 10^{-2} M leads to the appearance of lower-energy bands at 393 nm (III) and 436 nm (IV) with increasing intensities relative to band II. Figure 2c shows the emission spectra versus concentration using 315 nm excitation, which corresponds to the lowest-energy excitation band characteristic of the "largest" oligomers. The 10^{-5} M solution exhibits no luminescence under 315 nm excitation. The major emission bands exhibited by the 10^{-4} M solution are bands III and IV. The relative intensity of band IV increases as the concentration is increased further to 10^{-3} and 10^{-2} M, respectively. The results in Figure 2 clearly indicate a progressive increase in the relative intensities of the lower-energy bands relative to the higher-energy bands upon increasing the dicyanoaurate(I) concentration in methanol frozen solutions. These results indicate the formation of at least four luminescent $*[Au(CN)_2^-]_n$ oligomers.

2. Luminescence of $K[Ag(CN)_2]$ Solutions. Aqueous and methanolic solutions of $K[Ag(CN)_2]$ luminesce at ambient temperature only when the concentration is high ($\geq 10^{-1}$ M levels). The photoluminescence properties of these solutions do not change as drastically versus concentration as the analogous $K[Au(CN)_2]$ solutions do. For example, increasing the concentration from 0.500 to 1.00 M in aqueous $K[Ag(CN)_2]$ leads to the enhancement in the luminescence intensity with no shift in the peak position ($\lambda_{max} \sim 400$ nm). Furthermore, changing the excitation wavelength did not change the profile of the emission spectrum. Much more drastic changes have been obtained for frozen solutions.

Frozen solutions of $K[Ag(CN)_2]$ in methanol exhibit emission spectra that are dependent on the concentration and excitation wavelength. Representative examples are shown in Figure 3. The emission spectrum of the 0.0100 M solution with $\lambda_{exc} = 240$ nm shows two high-energy bands at ~300 nm (labeled A) and 340 nm (labeled B) with a stronger intensity for the 300 nm band. An increase of the $Ag(CN)_2^-$ concentration to 0.0500 M results in the disappearance of the 300 nm band while the 340 nm emission becomes dominant. A similar trend is observed when using $\lambda_{exc} = 260$ nm. Using this excitation wavelength, a new lower-energy emission band appears near 430 nm (labeled

(48) Nagasundaram, N.; Roper, G.; Biscoe, J.; Chai, J. W.; Patterson, H. H.; Blom, N.; Ludi, A. *Inorg. Chem.* **1986**, *25*, 2947.

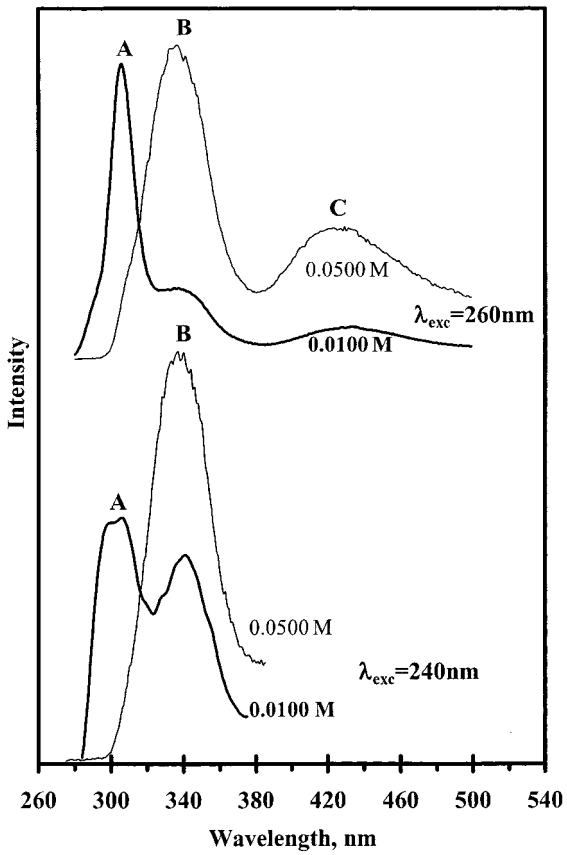

Figure 3. Emission spectra of $K[Ag(CN)_2]$ in methanol frozen solutions (77 K) versus concentration and excitation wavelength.

C), the relative intensity of which increases in the more concentrated solutions.

Frozen aqueous solutions exhibit strong luminescence with $Ag(CN)_2^-$ concentrations as low as 10^{-4} M. Figure 4 shows the emission spectra of these solutions versus concentration and excitation wavelength. The selection of the two excitation wavelengths is based on the excitation maxima. Two major emission bands appear in Figure 4, a higher-energy (HE) band near 350 nm and a lower-energy (LE) band near 400 nm. Interestingly, the intensity ratio of the LE/HE bands decreases upon increasing the concentration. This is an unusual result, because one would predict an opposite trend for layered species such as the dicyanoargentates(I) and dicyanoaurates(I). The luminescence bands for $Au(CN)_2^-$ show an increase in the intensity ratio of the LE/HE bands upon increasing the concentration of solutions (Figures 1 and 2). Solutions of layered cyano compounds of other metal ions such as Pt(II) also show an increase in the intensity ratio of the LE/HE bands upon increasing the concentration.[46,47] The unusual concentration dependence of the emission bands of $Ag(CN)_2^-$ aqueous solutions is because the HE emission is associated with a lower-energy excitation maximum than the one for the LE emission. The characteristic excitation wavelengths of the HE and LE emission bands are 290 and 260 nm, respectively. A similar observation has been reported for $Ag(CN)_2^-$/KCl doped crystals.[10] The unusual correlation between the emission and excitation band energies in $Ag(CN)_2^-$ can be explained by the model shown in Figure 5, which depicts how the lower-energy emission band C is associated with a higher-energy excitation transition than the one for band B. The model is based on quantum mechanical calculations for two different geometrical isomers of a $[Ag(CN)_2^-]_3$ trimer.

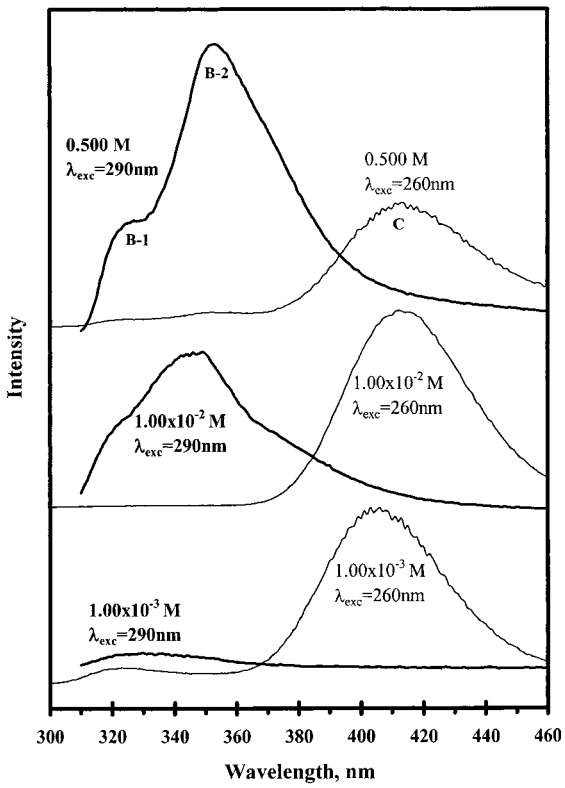

Figure 4. Emission spectra of $K[Ag(CN)_2]$ in aqueous frozen solutions (77 K) versus concentration and excitation wavelength.

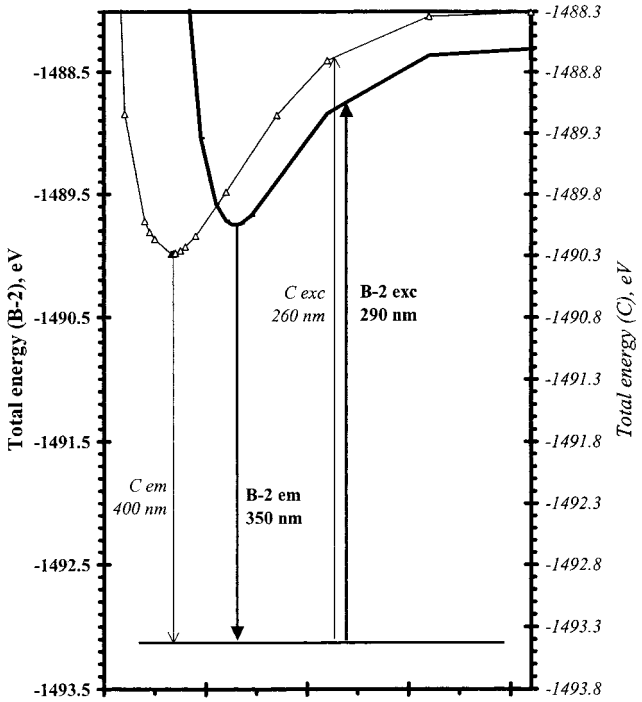

Figure 5. Potential energy diagrams of the excited states of the $[Ag(CN)_2^-]_n$ oligomers responsible for emission bands B and C. The energies are based on extended Hückel calculations for two geometrical isomers of a $[Ag(CN)_2^-]_3$ linear trimer (eclipsed and staggered conformations).

3. Metal−Metal Bonded Excimers and Exciplexes. In ref 33, the presence of various $[M(CN)_2^-]_n$ oligomers (M = Au, Ag) in solution has been demonstrated, and the formation constants and bond energies for these oligomers have been calculated on the basis of experimental and theoretical results.

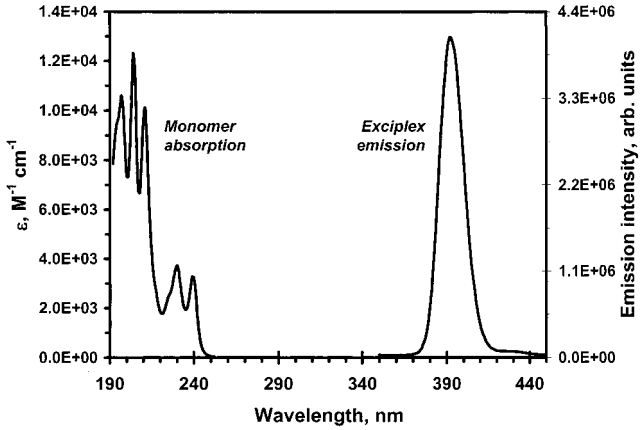

Figure 6. A comparison between the exciplex emission and the monomer absorption for the dicyanaurates (I). The monomer absorption is represented by the absorption spectrum of a 10^{-4} M solution of $K[Au(CN)_2]$ at ambient temperature, while the exciplex emission is represented by the emission spectrum of a $Au(CN)_2^-$/NaCl doped single crystal at 10 K.

Here, we characterize the M−M bonding in the first excited electronic state relative to the ground state. For the $[Ag(CN)_2^-]_n$ oligomers, it has been established[10,36] that the Ag−Ag distance decreases significantly upon photoexcitation, which results in a Ag−Ag single bond in the first excited state. Therefore, the multiple emissions observed for doped crystals of $Ag(CN)_2^-$ in alkali halide lattices have been assigned to $*[Ag(CN)_2^-]_n$ excimers ($n = 2$) and exciplexes ($n > 2$) that differ in "*n*" and/or geometry.[10] The emission bands observed here for $K[Ag(CN)_2]$ solutions are very similar in shape and energy to those exhibited by doped crystals of $Ag(CN)_2^-$ in alkali halide lattices. Therefore, the emission bands A−C (Figures 3 and 4) are assigned to different geometrical isomers of $*[Ag(CN)_2^-]_2$ excimers and $*[Ag(CN)_2^-]_3$ exciplexes. We believe that exciplex behavior also applies for the analogous $[Au(CN)_2^-]_n$ oligomers.

The exciplex assignment for the luminescence bands of the dicyanoaurates(I) is supported by the spectral observations we have made. The emission bands in Figures 1 and 2 are structureless, have large Stokes shifts, and are largely red-shifted from the monomer absorption bands. These are typical features of exciplex bands,[49] because they indicate a very large displacement of the excited state relative to the geometry of the ground state. It is important to note that these trends are valid not only for solutions but also for pure and doped crystals. The emission bands of the dicyanoaurates(I) are structureless even for doped single crystals of $Au(CN)_2^-$ at 10 K. Doping and cooling to low temperatures are methods typically used to improve the resolution and show structured emission in luminescent materials.[50] A typical emission spectrum of a $Au(CN)_2^-$/NaCl doped single crystal at 10 K is shown in Figure 6 and compared with the absorption spectrum of a dilute (10^{-4} M) solution. The structureless low-energy emission shown is in contrast to the highly structured high-energy absorption bands of the dilute solution, in which monomers dominate.

UMP2 calculations have been carried out for a staggered $[Au(CN)_2^-]_2$ dimer model in order to shed some light into the Au−Au bonding properties upon photoexcitation from the singlet ground state to the lowest-lying triplet excited state. The emission bands for the dicyanoaurates(I) have shown microsecond-level lifetimes, corresponding to triplet excited states.[48] Figure 7 shows contour plots of the two pertinent molecular orbitals involved in the lowest energy emission according to UMP2 calculations. Note that the Au−Au bonding character is antibonding (σ^*) in the HOMO and bonding (σ) in the LUMO (the HOMO and LUMO here refer to the definitions based on the singlet ground state; both orbitals are singly occupied in the triplet and singlet excited states). Therefore, exciplex formation in the dicyanoaurates(I) may take place as a result of a HOMO−LUMO Au-centered excitation transition from an antibonding orbital to a bonding orbital. Full UMP2 optimization for the triplet excited state leads to a geometry in which the Au−Au equilibrium distance is 2.66 Å. This distance is exceptionally short, in comparison to ground-state Au(I) species, and it corresponds to a Au−Au singly bonded excimer, $*[Au(CN)_2^-]_2$. The 2.66 Å Au−Au distance in the $*[Au(CN)_2^-]_2$ excimer is well within the range of typical Au−Au single bond distances in structurally determined Au(II) compounds[51,52] (e.g., 2.67 Å in $[Au(CH_2)_2PPh_2]_2(CH_3)Br$[51a] and 2.61 Å in $[Au(dppn)Cl]_2(PF_6)_2$,[51b] where dppn = 1,8-bis(diphenylphosphino)naphthalene). We have carried out frequency calculations at the MP2 level in order to further characterize the Au−Au bonding in the $*[Au(CN)_2^-]_2$ excimer and the $[Au(CN)_2^-]_2$ ground-state dimer. The results are summarized in Table 1. It is noted that the excited-state distortion is associated with Au−Au bonding, as the Au−C and C−N distances are only slightly different in the excimer relative to the ground-state values. Table 1 shows that, on going from the dimer to the excimer, the Au−Au stretching frequency undergoes a significant increase, from ∼90 to 166 cm^{-1}, the force constant increases by an order of magnitude, and the reduced mass increases from ∼31 to 122. All these results clearly illustrate a dramatic increase in Au−Au bonding in the triplet excimer relative to the aurophilically bonded ground-state dimer.

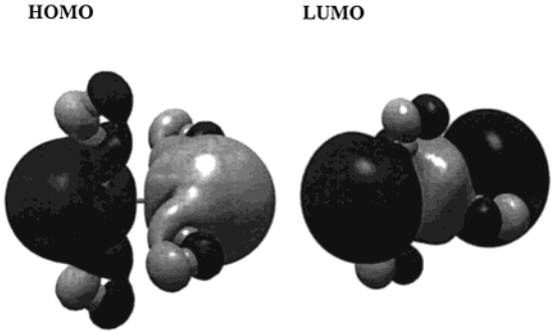

Figure 7. Contour diagrams (isodensity value = 0.02) for the HOMO and LUMO of a staggered $[Au(CN)_2^-]_2$ dimer model according to UMP2 calculations.

Extended Hückel (EH) calculations give similar bonding properties for the HOMO and LUMO of $[Au(CN)_2^-]_n$ oligomers.

(49) (a) *The Exciplex*; Gordon, M., Ware, W. R., Eds; Academic Press: New York, 1975. (b) Omary, M. A.; Patterson, H. H. Electronic Spectroscopy: Luminescence Theory. *Encyclopedia of Spectroscopy & Spectrometry*; Academic Press: London, U.K., 2000; pp 1186−1207.

(50) Zink, J. I.; Shin, K. S. K. Molecular Distortions in Excited Electronic States Determined from Electronic and Resonance Raman Spectroscopy. In *Advances in Photochemistry*; Volman, D. H., Hammond, G. S., Neckers, D. C., Eds.; Wiley: New York, 1991; Vol. 16.

(51) (a) Basil, J. D.; Murray, H. H.; Fackler, J. P., Jr.; Tocher, J.; Mazany, A. M.; Trzcinska-Bancroft, B.; Knachel, H.; Dudis, D.; Delord, T.-J.; Marler, D. O. *J. Am. Chem. Soc.* **1985**, *107*, 6908. Au−Au distances of 2.55−2.65 Å have been reported in a variety of organometallic gold(II) complexes. For a recent overview, see: Carlson, T. F.; Fackler, J. P., Jr. *J. Organomet. Chem.* **2000**, 596, 237. (b) Yam, V. W. W.; Choi, S. W. K.; Cheung, K. K. *Chem. Commun.* **1996**, 1173. This reference is the only example reported for ligand-unsupported Au(II)−Au(II) bonding.

(52) For reviews, see: (a) Laguna, A.; Laguna, M. *Coord. Chem. Rev.* **1999**, *193−195*, 837. (b) Grohmann, A.; Schmidbaur, H. In *Comprehensive Organometallic Chemistry II;* Abel, E. W., Stone, F. G. A., Wilkinson, G., Eds.; Pergamon: Oxford, 1995; Vol. 3, Chapter 1.

Table 1. Summary of MP2 Frequency Calculations for the Electronic Ground State and First Excited Triplet State of Staggered $[Au(CN)_2^-]_2$[a]

electronic state	d(Au−Au),Å	d(Au−C), Å	d(C−N), Å	ν_{Au-Au}, cm^{-1}	k(Au−Au), mDyne/A	μ(Au−Au)
ground state	2.960	2.018	1.197	89.8	0.1470	30.94
triplet excited state	2.664	2.012	1.183	165.7	1.9729	121.98

[a] Notation used: d(X−Y), equilibrium interatomic distance between X and Y; ν_{Au-Au}, stretching frequency for the Au−Au bond; k(Au−Au), force constant for the Au−Au bond; μ(Au−Au), reduced mass for the vibrational mode assigned to ν_{Au-Au}.

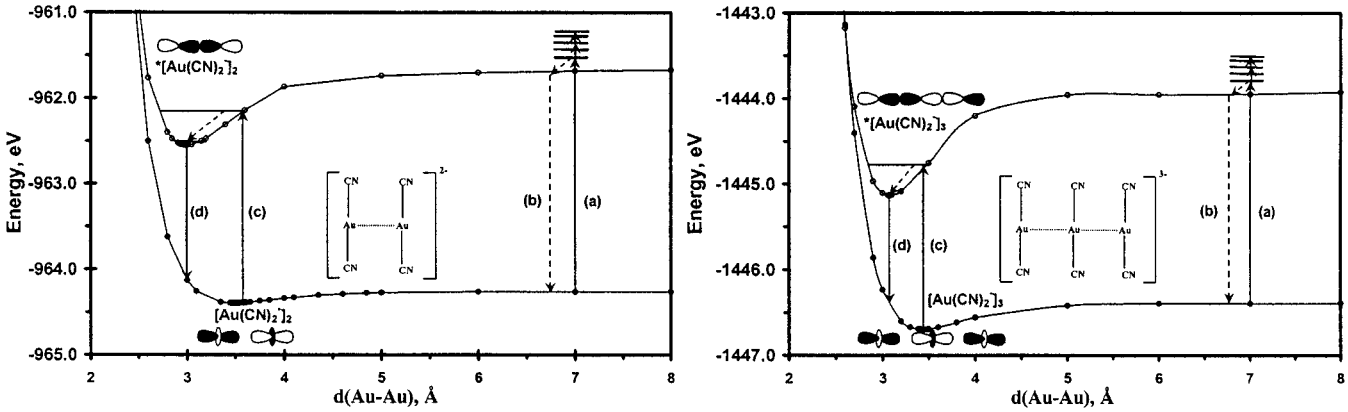

Figure 8. Ground and excited-state calculations for eclipsed isomers of $[Au(CN)_2^-]_2$ (left) and $[Au(CN)_2^-]_3$ (right). Optical transitions are labeled: (a) dilute solution absorption, (b) nonradiative relaxation, (c) concentrated solution absorption, and (d) excimer emission (left) and trimer exciplex emission (right).

The HOMO is an antibonding orbital consisting mostly of $5d_{z^2}$ orbitals but with significant mixing (∼30%) from 6s orbitals, while the LUMO is a bonding orbital consisting mostly of $6p_z$ orbitals. Because of the qualitative similarity between the MP2 and EH calculations, calculations were carried out using the EH method for both the ground and first excited electronic states of various $[Au(CN)_2^-]_n$ oligomers ($n = 2, 3$) with a variety of possible conformations and geometries (eclipsed and staggered for all oligomers; linear and bent trimers). The Au−Au distance between monomer anions in each oligomer was optimized (varied between 1 and 8 Å) with the EH calculations.

Figure 8 shows representative examples summarizing the results of EH calculations for eclipsed isomers of a $[Au(CN)_2^-]_2$ dimer (D_{2h}) and a $[Au(CN)_2^-]_3$ linear trimer (D_{2h}) in both the ground and first excited electronic states. The results show that, for a given $[Au(CN)_2^-]_n$ oligomer, the first excited electronic state has a deeper potential well (higher binding energy) and a shorter Au−Au equilibrium distance than the ground state. For example, the eclipsed dimer has a binding energy of ∼0.1 eV and Au−Au distance of ∼3.5 Å in the ground state (Figure 8). In the first excited state, these values change to ∼0.9 eV and 3.0 Å. Figure 8 also shows that the Au−Au bonding in both the ground and first excited state is stronger in the trimer than in the corresponding dimer. Similar calculations have been carried out for the staggered $[Au(CN)_2^-]_2$ dimer, staggered $[Au(CN)_2^-]_3$ linear trimer, and eclipsed $[Au(CN)_2^-]_3$ bent trimer (symmetries are D_{2d}, D_{2h}, and C_{2v}, respectively). See the structures in Chart 1. These calculations have shown similar qualitative trends to the ones shown in Figure 8. It is, therefore, concluded that, for all $[Au(CN)_2^-]_n$ oligomers, Au−Au bonding is stronger in the first excited state than in the ground state. This conclusion should not be surprising, because Au(I) has a closed-shell electronic configuration in the ground state ($5d^{10}$), while the excited state has an open-shell configuration ($5d^96s^1$). The mixing of the 6s and/or 6p orbitals with the 5d orbitals contributes to the ground-state aurophilic bonding, because of correlation effects and the strong relativistic effects of gold.[8] However, such a ground-state bonding is relatively weak, with an average of ∼35 kJ/mol according to several experimental and theoretical studies.[33,53−56] The fact that the calculations here indicate much stronger Au−Au bonding in the first excited state relative to the ground state is indicative of the formation of $*[Au(CN)_2^-]_n$ excimers and exciplexes.

The optical transitions depicted in Figure 8 correlate nicely with the experimental spectra shown in Figure 6, in a manner similar to that proposed in textbooks for organic excimers and exciplexes.[49,57] The monomer absorption seen at low $Au(CN)_2^-$ concentration is highly structured and occurs at high energies (transition "a"). Corresponding structured emissions were not observed experimentally, thus monomers are not luminescent (transition "b"). The absorption and excitation bands for concentrated solutions[33] (and in the solid state[58]) are red-shifted (transition "c") from the monomer absorption bands. Following lattice relaxation, excimer/exciplex emissions occur (transition "d") with their characteristic low energies and structureless profiles (Figure 6). The low energies of the excimer/exciplex emissions are explained in Figure 8, as transition "d" occurs from a largely stabilized excited state to a destabilized ground state. The absence of structure is also explained, as transition "d", because of the large excited-state distortion, terminates on the vacuum region of the ground state where nuclear repulsion dominates. In the absence of a large excited-state distortion, a

(53) (a) Jones, W. B.; Yuan, J.; Narayanaswamy, R.; Young, M. A.; Elder, R. C.; Bruce, A. E.; Bruce, M. R. M. *Inorg. Chem.* **1995**, *34*, 1996. (b) Narayanaswamy, R.; Young, M. A.; Parkhurst, E.; Ouellette, M.; Kerr, M. E.; Ho, D. M.; Elder, R. C.; Bruce, A. E.; Bruce, M. R. M. *Inorg. Chem.* **1993**, *32*, 2506.

(54) Harwell, D. E.; Mortimer, M. D.; Knobler, C. B.; Anet, F. A. L.; Hawthorne, M. F. *J. Am. Chem. Soc.* **1996**, *118*, 2679.

(55) (a) Zank, J.; Schier, A.; Schmidbaur, H. *J. Chem. Soc., Dalton Trans.* **1998**, 323. (b) Schmidbaur, H.; Graf, W.; Müller, G. *Angew. Chem., Int. Ed. Engl.* **1988**, *27*, 417.

(56) Tang, S. S.; Chang, C. P.; Lin, I. J. B.; Liou, L. S.; Wang, J. C. *Inorg. Chem.* **1997**, *36*, 2294.

(57) An important difference between Au−Au bonded exciplexes and organic exciplexes is that the ground state has a shallow minimum due to aurophilic bonding in Au−Au bonded exciplexes while organic exciplexes are assumed to have a nonbonding ground state. See: Turro, N. J. *Modern Molecular Photochemistry*; Benjamin/Cummings: Melano Park, CA, 1978; pp 135−146.

(58) Rawashdeh-Omary, M. A. Ph.D. Thesis, Graduate School, University of Maine, 1999.

Table 2. Summary of the Results of Extended Hückel Calculations for the Ground and Excited Electronic States of Oligomeric Species of Dicyanoaurate (I)

species[a]	[Au]	$[Au]_2$ (ecl)	$*[Au]_2$ (ecl)	$[Au]_2$ (st)	$*[Au]_2$ (st)	$[Au]_3$ (ecl, bent)	$*[Au]_3$ (ecl, bent)	$[Au]_3$ (ecl, lin)	$*[Au]_3$ (ecl, lin)
Au−Au eq dist,[b] Å	8.00[e]	3.48	3.00	2.88	2.47	3.48	3.15	3.44	3.08
binding energy, eV	0.00	0.132	0.877	0.298	1.19	0.266	0.877	0.301	1.21
H−L gap,[c] eV	4.41	3.78	3.41	3.59	3.35	3.62	3.30	3.43	2.96
O. P.[d] (Au−Au)	0.000	0.0226	0.0734	0.0703	0.120	0.0203	0.0679	0.0116	0.569

[a] Notation: $[Au]_n = [Au(CN)_2^-]_n$, $*[Au]_n$ = excimer/exciplex, ecl = eclipsed, st = staggered, bent = bent trimer, lin = linear trimer. See Chart 1 for structures. [b] Eq dist = equilibrium distance. [c] HOMO−LUMO gap. [d] O. P. = overlap population. Values listed for bonds with the central gold atom. [e] Isolated ions are considered at an Au−Au distance of 8 Å, at which the total energy reaches a plateau (see Figure 8).

structured emission is normally observed. For example, several luminescent 2-coordinate Au(I) complexes have been reported to show structured emissions, especially for crystalline materials at cryogenic temperatures. Mononuclear,[59] dinuclear,[60] and trinuclear[61,62] Au(I) compounds showing these emission properties have been reported. In these examples, the ligand orbitals are involved in the ground state, and small Stokes shifts are observed, indicative of small excited-state distortions and, thus, accounting for the structured emissions with progressions in ligand vibrations. In contrast, luminescent 3-coordinate Au(I) mononuclear compounds exhibit structureless emissions with large Stokes shifts assigned to transitions between Au(I) orbitals that are largely distorted because of the AuP_3 coordination mode.[5,30,63] An interesting example has been reported in which two emissions are observed: a structured ligand-to-metal charge-transfer emission and a structureless Au-centered emission that is sensitive to Au−Au separation.[64]

A plethora of studies for luminescent complexes of Au(I) have reported Au-centered emissions from a bonding LUMO to an antibonding HOMO as the transitions responsible for the low-energy luminescence.[64−69] Despite this assignment and the fact that the emission profiles of the low-energy luminescence bands in all these examples show the typical features of excimer/exciplex bands (structureless emission, large Stokes shift), there was no mention of Au−Au bonded excimers and exciplexes in any of these studies, possibly because of the lack of evidence showing the formation of a bona fide Au−Au bond in the excited state. Recently, however, Che et al. have presented the first experimental evidence, based on resonance Raman results, showing the formation of an *intramolecular* Au−Au single bond in the excited state of a bimolecular Au(I) complex, in which the two gold atoms are bridged by a diphosphino ligand.[70] However, the low energy luminescence bands for this class of compounds was attributed to an exciplex bond between the gold complex and either a solvent or a counterion,[71] not an *intermolecular* metal−metal excimer/exciplex bond like the case here for the dicyanoaurates(I). It has been suggested that an intramolecular Au−Au bond in bimolecular Au(I) compounds does not lead to the extremely low emission energies observed experimentally.[70,71] The situation is different here for several reasons. First, the stabilization due to intermolecular exciplex formation of $*[Au(CN)_2^-]_n$ is large enough to explain the emission energies, and a good correlation is established between the experimental and theoretical results (vide infra). Second, an exciplex involving the solvent is ruled out, because the emission bands in solution and the solid state are very similar in shape and energy.[58] Third, an exciplex involving the countercation is also ruled out, because virtually identical emission energies were obtained for dicyanoaurate(I) (and dicyanoargentate(I)) species with different counterions (e.g., K^+ vs Na^+).[58]

Table 2 summarizes the results of ground- and excited-state EH calculations for the various $[Au(CN)_2^-]_n$ oligomers shown in Chart 1. The Au−Au bond energies and distances are dependent upon the number of ions in the oligomer (dimers vs trimers), their geometry (linear vs bent trimers), and conformation (eclipsed vs staggered dimers). Nevertheless, all oligomers show stronger Au−Au bonding in the first excited state relative to the ground state, as indicated by shorter Au−Au equilibrium distances, greater binding energies, and higher Au−Au overlap populations. The strongest Au−Au bonding occurs in staggered isomers. For the staggered $[Au(CN)_2^-]_2$ dimer, the Au−Au bond energy increases from 30 kJ/mol in the ground state to 115 kJ/mol in the first excited state. The value of the Au−Au bond energy in the first excited state is comparable with the bond energies of many metal−metal single bonds.[72] This is a further indication for the formation of an actual "Au−Au bond" in the first excited state, as opposed to the weaker "Au−Au interactions" in the ground state.

4. Comparison of Ground- and Excited-State Au−Au and Ag−Ag Bonding. The formation of excimers and exciplexes for the dicyanoaurates(I) and dicyanoargentates(I) is a result of excited-state Au−Au and Ag−Ag bonding interactions, respectively. Here, we would like to compare excited-state bonding versus ground-state bonding for $[Au(CN)_2^-]_n$ and $[Ag(CN)_2^-]_n$ oligomers. The models used for this comparison are staggered isomers of dimers and trimers in order to minimize attractive and repulsive forces involving the ligands (e.g., steric repulsion, van der Waals, or hyperconjugation attraction forces).[73]

(59) Larson, L. J.; McCauley, E. M.; Weissbart, B.; Tinti, D. S. *J. Phys. Chem.* **1995**, *99*, 7218.
(60) Hanna, S. D.; Zink, J. I. *Inorg. Chem.* **1996**, *35*, 297.
(61) Hanna, S. D.; Khan, S. I.; Zink, J. I. *Inorg. Chem.* **1996**, *35*, 5813.
(62) Burini, A.; Fackler, J. P., Jr.; Galassi, R., Grant, T. A.; Omary, M. A.; Rawashdeh-Omary, M. A.; Pietroni, B. R.; Staples, R. J. *J. Am. Chem. Soc.* **2000**, *122*, 11264.
(63) McClesky, T.; Gray, H. B. *Inorg. Chem.* **1992**, *31*, 1733.
(64) Assefa, Z.; McBurnett, B. G.; Staples, R. J.; Fackler, J. P., Jr. *Inorg. Chem.* **1995**, *34*, 4965.
(65) Assefa, Z.; McBurnett, B. G.; Staples, R. J.; Fackler, J. P., Jr.; Assmann, B.; Angermaier, K.; Schmidbaur, H. *Inorg. Chem.* **1995**, *34*, 75.
(66) Weissbart, B.; Toronto, D. V.; Balch, A. L.; Tinti, D. S. *Inorg. Chem.* **1996**, *35*, 2490.
(67) King, C.; Wang, J.-C.; Khan, Md. N. I.; Fackler, J. P., Jr. *Inorg. Chem.* **1989**, *28*, 2145.
(68) (a) Jaw, H.-R. C.; Savas, M. M.; Rogers, R. D.; Mason, W. R. *Inorg. Chem.* **1989**, *28*, 1028. (b) Jaw, H.-R. C.; Savas, M. M.; Mason, W. R. *Inorg. Chem.* **1989**, *28*, 4366.
(69) Fernandez, E. J.; Gimeno, M. C.; Laguna, A.; Lopez-de-Luzuriaga, J. M.; Monge, M.; Pyykkö; P.; Sundholm, D. *J. Am. Chem. Soc.* **2000**, *122*, 7287.
(70) Leung, K. H.; Phillips, D. L.; Tse, M. C.; Che, C. M.; Miskowski, V. M. *J. Am. Chem. Soc.* **1999**, *121*, 4799.
(71) Fu, W. F.; Chan, K. C.; Miskowski, V. M.; Che, C. M. *Angew. Chem., Int. Ed. Engl.* **1964**, *38*, 2783.
(72) Cotton, F. A.; Walton, R. A. *Multiple Bonds between Metal Atoms*, 2nd ed.; Clarendon Press: Oxford, 1993.
(73) The eclipsed geometry also allows for excited-state interactions between adjacent cyanide groups, which may contribute to the binding energies for $*[Au(CN)_2^-]_2$ and $*[Au(CN)_2^-]_3$. Estimations of the excited-state metal−metal bond energies are, therefore, better drawn from calculations for staggered isomers.

Table 3. Comparison of Gold−Gold Interactions versus Silver−Silver Interactions Based on Extended Hückel Calculations for Staggered Models of $[M(CN)_2^-]_2$ and $[M(CN)_2^-]_3$ (M = Au, Ag)[a]

	ground-state calculations			excited-state calculations			
system	binding energy, eV	M−M bond energy, eV	M−M bond energy, kJ/mol	binding energy, eV	Δq, Å[b]	M−M bond energy, eV	M−M bond energy, kJ/mol
$[Au(CN_2^-]_2$	0.298	0.298	30	1.19	−0.41	1.19	115
$[Ag(CN)_2^-]_2$	0.218	0.218	21	1.32	−0.49	1.32	127
$[Au(CN)_2^-]_3$	0.707	0.353	34	1.90	−0.28	0.950	92
$[Ag(CN)_2^-]_3$	0.612	0.306	30	2.00	−0.33	1.00	97

[a] Values for $[Ag(CN)_2^-]_n$ species are taken from reference 10. [b] Δq is the excited-state distortion calculated as the difference between the M−M equilibrium distance in the excited state and the corresponding equilibrium distance in the ground state.

The ground-state MP2 calculations for staggered $[Au(CN)_2^-]_2$ gave rise to an Au−Au equilibrium distance of 2.96 Å. This distance is slightly longer than the Au−Au distance in metallic gold (2.89 Å) and similar to Au−Au distances in many Au(I) complexes. However, it is somewhat shorter than Au−Au distances in pure crystals of $M[Au(CN)_2]$, typically 3.1−3.6 Å. The packing in the two-dimensional layers of the solids as well as the presence of counterions are factors that exist in the solids, but they are not accounted for in the MP2 calculations for the dianionic staggered model of $[Au(CN)_2^-]_2$. Dolg et al. have presented a similar argument about the effect of intermolecular interactions and charge on the closed-shell Tl−Pt interactions in $Tl_2[Pt(CN)_4]$.[74] The absence of these factors in a simple $Tl_2[Pt(CN)_4]$ gas-phase model has led to a calculated Tl−Pt distance of 2.877 Å (MP2 method), significantly shorter than the crystallographic value of 3.140 Å for the packed solid. The equilibrium Au−Au distance in $[Au(CN)_2^-]_2$ decreases from 2.96 Å in the ground state to 2.66 Å in the lowest-energy triplet excited state, representing an excited-state distortion (Δq) of −0.30 Å. A recent resonance Raman study by Che and coworkers for $[Au_2(dcpm)_2](ClO_4)_2$, dcpm = dicyclohexylphosphinomethane, has also shown significant reduction in the Au−Au distance from 2.92 Å in the ground state to 2.80 Å in the first excited state.[70]

We use EH calculations to compare Au−Au and Ag−Ag bonding in the ground and excited states for dimer and trimer models. Table 3 includes calculated values for the excited-state distortion from EH calculations. The negative values of Δq suggest that oligomers of both the dicyanoaurate(I) and dicyanoargentate(I) ions exhibit a reduction in the metal−metal equilibrium distances upon photoexcitation. The large excited-state distortions shown in Table 3 explain the large Stokes shifts for the luminescence bands. The negative shift in Δq is greater for the Ag(I) oligomers than the corresponding Au(I) oligomers. This is in accordance with higher metal−metal bond energies in the excited state for Ag−Ag bonds than for Au−Au bonds, as shown by EH calculations. This is an interesting prediction, because it shows an opposite trend relative to that of the ground-state bond strength, in which Au−Au bonds are stronger. This unexpected trend predicted at the EH level is supported by experimental results for dinuclear Au(I) and Ag(I) compounds, which have reproduced the same trend. Che et al. have recently reported a Δq of −0.20 Å for $[Ag_2(dcpm)_2]^{2+}$,[75] compared to a −0.12 value for $[Au_2(dcpm)_2]^{2+}$,[70] as determined by resonance Raman spectroscopy and intensity analysis methods.

Table 3 shows that the excited-state Ag−Ag bond is stronger than the corresponding Au−Au bond by 12 kJ/mol in dimer models and by 5 kJ/mol in trimer models. By taking the average of the dimer and trimer values, the excited-state Ag−Ag and Au−Au bond energies are 112 and 104 kJ/mol, respectively. These values represent much stronger metal−metal bonding in the first excited states relative to the ground states for both Ag(I) and Au(I). The metal−metal bonding is stronger in the first excited state than in the ground state by 4.4 times for Ag(I) and 3.3 times for Au(I). Table 3 indicates a cooperativity effect for the ground-state metal−metal bonding in staggered oligomers, with the metal−metal bond energies higher for trimers than for dimers. This effect has also been confirmed experimentally in ref 33. However, the excited-state metal−metal bond energies in Table 3 are higher for dimers than for trimers, suggesting that the cooperativity of Au−Au and Ag−Ag bonding is not enhanced upon photoexcitation of the staggered isomers.

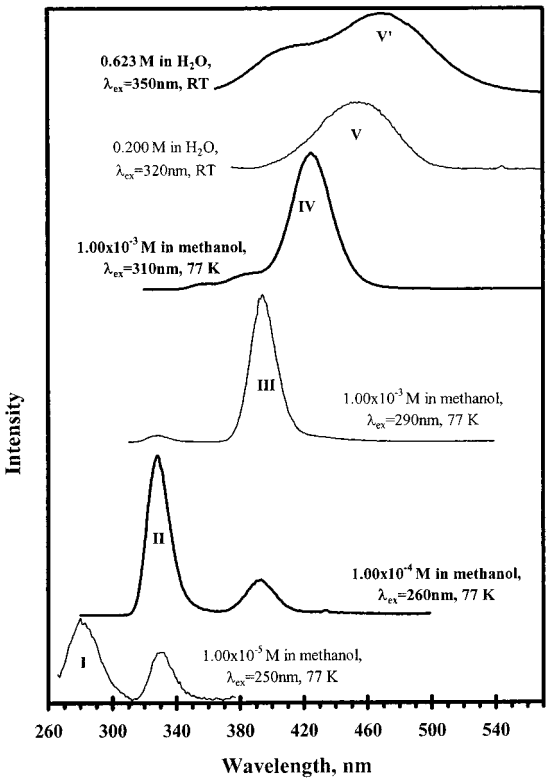

Figure 9. Tunable emission of $K[Au(CN)_2]$ solutions by controlling the concentration, excitation wavelength, solvent, and temperature.

5. Tunable Photoluminescence. The results here indicate large tunabilities in the excited states for the dicyanoaurate(I) and dicyanoargentate(I) species. This is illustrated by the appearance of multiple emission bands, the energies and intensities of which can be controlled (or *tuned*) by a variety of factors such as changing the solute concentration, excitation wavelength, temperature, and solvent. The tunable luminescence of $Au(CN)_2^-$ in solution is illustrated in Figure 9. Five distinct emission bands appear in the luminescence spectra of aqueous

(74) Dolg, M.; Pyykkö, P.; Runeberg, N. *Inorg. Chem.* **1996**, *35*, 7450.

(75) Che, C. M.; Tse, M. C.; Chan, M. C. W.; Cheung, K. K.; Phillips, D. L.; Leung, K. H. *J. Am. Chem. Soc.* **2000**, *122*, 2464.

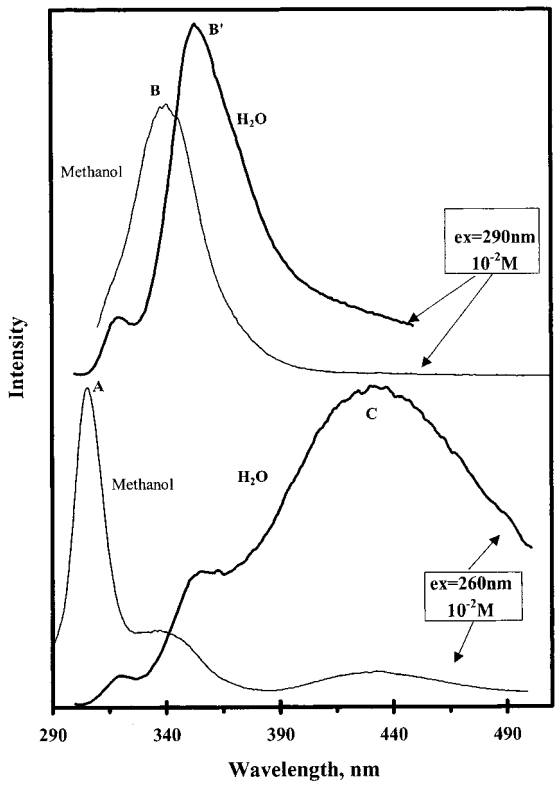

Figure 10. Tunable emission of $K[Ag(CN)_2]$ in aqueous versus methanolic solutions at 77 K.

and methanolic solutions of $K[Au(CN)_2]$. These bands are labeled in Figure 9, in order of decreasing energy, as I, II, III, IV, and V. A typical luminescence spectrum of $K[Au(CN)_2]$ consists of two or more emission bands that often overlap with each other. One can control the excitation wavelength, temperature, concentration, and solvent to resolve and/or maximize the appearance of a particular emission band. This is illustrated in the spectra shown in Figure 9. For example, the highest-energy band (I) is observed only in the lowest-concentration limit at which $Au(CN)_2^-$ luminescence is observed (10^{-5} M levels). The emission spectrum of a frozen solution with this concentration shows band I when excited with a short excitation wavelength. On the other hand, the appearance of the lowest-energy emission band (V) can be maximized by the opposite conditions: high concentration ($\geq$0.2 M), long excitation wavelengths (>300 nm), and a higher temperature (ambient). *Fine-tuning* of the luminescence within the energy range of one particular luminescence band can also be achieved. This can be accomplished by small variations of concentration and excitation wavelengths. For example, a progressive change in the $K[Au(CN)_2]$ concentration, between 0.200 and 0.623 M, and excitation wavelength, between 320 and 350 nm, gives rise to a fine-tuning of the emission peak position between 455 nm (V) and 470 nm (V′) at ambient temperature.

Tunable photoluminescence for $Ag(CN)_2^-$ species in the solid state is now well established.[7,10,37,38] The emission can be tuned by site-selective excitation to bands with peak maxima near 290 (A), 310 (B-1), 350 (B-2), 400 (C), and 500 nm (D) in a variety of pure and doped crystals. We show here that $Ag(CN)_2^-$ solutions also exhibit tunable photoluminescence, by variation of the concentration, solvent, temperature, and excitation wavelength. Figure 10 illustrates the tunable luminescence of $Ag(CN)_2^-$ by comparing the spectra of aqueous versus methanolic solutions of $K[Ag(CN)_2]$ under similar conditions of concentration, temperature, and excitation wavelength. Three

Table 4. Assignment of the Emission Bands Observed in Solutions of $KAu(CN)_2$ and $KAg(CN)_2$

[Au] bands	λ_{max}^{em}, nm[a]	assignment	[Ag] bands	λ_{max}^{em}, nm[a]	assignment
I	275−285	$*[Au(CN)_2^-]_2$	A	290−305	$*[Ag(CN)_2^-]_2$
II	320−350	$*[Au(CN)_2^-]_3$[b]	B-1	315−330	$*[Ag(CN)_2^-]_3$[b]
III	380−390	$*[Au(CN)_2^-]_3$[b]	B-2	345−360	$*[Ag(CN)_2^-]_3$[b]
IV	420−440	$*[Au(CN)_2^-]_{n_1}$[c]	C	410−440	$*[Ag(CN)_2^-]_3$[b]
V	455−470	$*[Au(CN)_2^-]_{n_2}$[c]			

[a] The exact band maximum is dependent on the solvent, temperature, and concentration. [b] Different geometrical isomers (linear, bent) and conformers (eclipsed, staggered) of the trimer (see text). [c] $*[Au(CN)_2^-]_{n_1}$ and $*[Au(CN)_2^-]_{n_2}$ with $n_2 > n_1$.

major emission bands are displayed by aqueous and methanolic solutions of $K[Ag(CN)_2]$. These bands are labeled in Figure 10, in order of decreasing energy, as A, B, and C, respectively. There is a large difference in the photoluminescence behavior between aqueous and methanolic solutions of $K[Ag(CN)_2]$ at 77 K. The energies of the dominant $Ag(CN)_2^-$ luminescence bands in frozen methanol solutions are generally higher than those of the corresponding bands obtained in frozen aqueous solutions with similar concentrations. For example, the highest-energy band (A) shown in Figure 10 at ~300 nm in the methanol solution (λ_{exc} = 260 nm) does not appear in aqueous solutions with a similar $Ag(CN)_2^-$ concentration. A lower energy band (C) with λ_{max} ~430 nm dominates the emission spectrum of the analogous aqueous solution. In fact, band A does not appear even in the most dilute aqueous solutions of $K[Ag(CN)_2]$ that exhibit luminescence. Figure 10 shows that $K[Ag(CN)_2]$ frozen aqueous solutions exhibit lower-energy emission maxima than those in analogous methanolic solutions for the spectra obtained with λ_{exc} = 290 nm. Aqueous solutions of $K[Ag(CN)_2]$ luminesce with concentration levels as low as 10^{-4} M at 77 K while analogous methanolic solutions luminesce only when the concentration levels are $\geq 10^{-2}$ M. These solvent trends are also valid for $K[Au(CN)_2]$ solutions and may be attributed to the greater molar absorptivities of $Au(CN)_2^-$ and $Ag(CN)_2^-$ species in water than in methanol,[33] which can be attributed to a higher dipole strength in the more polar solvent, water.

The results in Table 2 show that the Au−Au bonding in $[Au(CN)_2^-]_n$ oligomers is sensitive to the number of interacting ions "*n*" (e.g., dimers vs trimers), as well as to the geometry (e.g., linear vs bent trimers) and configuration (e.g., eclipsed vs staggered) of a given oligomer. Because EH calculations show that these factors strongly affect the HOMO−LUMO gaps, different absorption and emission energies are expected to exist for $[Au(CN)_2^-]_n$ oligomers that differ in "*n*", geometry, or configuration. This is consistent with the optical data, as solutions of the dicyanoaurates(I) and dicyanoargentates(I) with different concentrations show multiple absorption (ref 33) and emission (Figures 1−4, 9, 10) bands. Table 4 provides a general summary for the luminescence bands observed in $KAu(CN)_2$ and $KAg(CN)_2$ solutions. The same trends discussed earlier[10] for the dicyanoargentates(I) are also relevant for the dicyanoaurates(I); hence, the reader is referred to ref 10 for details about the assignments. Multiple excitation and emission bands are also observed in doped and pure crystals of both the dicyanoaurates(I) and dicyanoargentates(I) because of the different oligomer sites in these solids.[7,10,36−38,48,58,76] The optical transitions responsible for the luminescence of $Au(CN)_2^-$ and $Ag(CN)_2^-$ solutions are

(76) (a) Markert, J. T.; Blom, N.; Roper, G.; Perregaux, A. D.; Nagasundaram, N.; Corson, M. R.; Ludi, A.; Nagle, J. K.; Patterson, H. H. *Chem. Phys. Lett.* **1985**, *118*, 258. (b) Assefa, Z.; DeStefano, F.; Garepapaghi, M. A.; LaCasce, J. H., Jr.; Ouellette, S.; Corson, M. R.; Nagle, J. K.; Patterson, H. H. *Inorg. Chem.* **1991**, *30*, 2868.

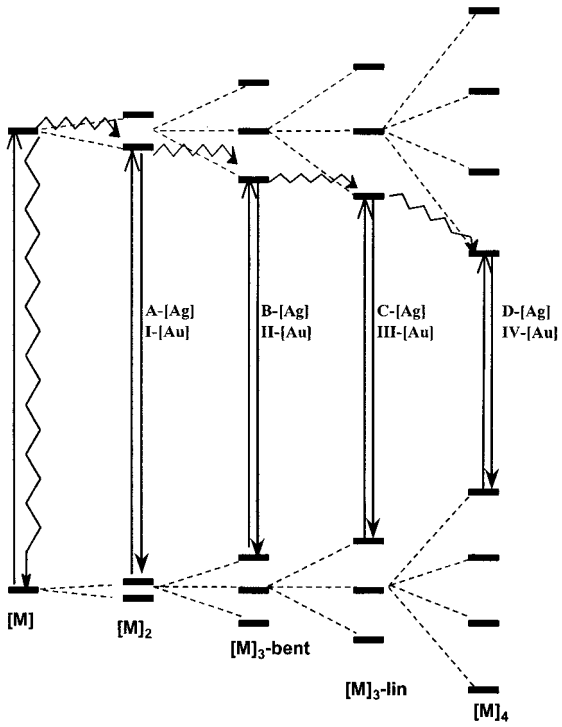

Figure 11. Optical transitions in $[Au(CN)_2^-]$ and $[Ag(CN)_2^-]$ systems. Solid and wiggled arrows represent radiative and nonradiative processes, respectively. Note that upon oligomerization the splitting of the excited states is greater than that in the ground state.

summarized in Figure 11. The excitation and emission transitions decrease in energy upon the formation of oligomers according to the trends in Table 2 discussed above. The appearance of a given oligomer band is due to either direct excitation of that oligomer or energy transfer from other oligomers. These processes and the factors affecting them (e.g., temperature, concentration, excitation wavelength) have been discussed elsewhere.[10,12,37,38]

The observation of multiple emission bands due to metal−metal bonded homoatomic excimers and exciplexes is unprecedented in the literature of Au(I) coordination compounds and reported only by the Patterson group for Ag(I) complexes. To our knowledge, the only precedents to our studies for such a behavior in inorganic systems are the spectroscopic studies of mercury in the gas phase.[77,78] The energy difference in the emission maxima between the $*Hg_2$ excimer and $*Hg_3$ linear trimer exciplex of mercury vapor is very similar ($9-10 \times 10^3$ cm^{-1}) to our experimental values (inferred from Table 4) for the corresponding excimers and exciplexes of the dicyanoaurates(I) and dicyanoargentates(I).

Conclusions

This study presents experimental and theoretical evidence relating the luminescence bands of Au(I) compounds to ligand-unsupported Au−Au bonds in the lowest excited state, as shown by modern ab initio calculations for the first time. MP2 calculations show that the equilibrium Au−Au distance in staggered $[Au(CN)_2^-]_2$ decreases from 2.96 Å in the ground state to 2.66 Å in the lowest-energy triplet excited state, thus suggesting the formation of a gold−gold single bond upon photoexcitation. Solutions of $K[Au(CN)_2]$ and $K[Ag(CN)_2]$ show multiple photoluminescence bands with shapes and energies suggesting their assignment to excimers and exciplexes. The emission bands are structureless and have extremely large Stokes shifts, indicating very large excited-state distortion consistent with excimer/exciplex emissions. The individual emission bands are assigned to metal−metal bonded $*[Au(CN)_2^-]_n$ and $*[Ag(CN)_2^-]_n$ excimers and exciplexes that differ in "*n*" and geometry. Metal−metal interactions in the first excited states of both $[Au(CN)_2^-]_n$ and $[Ag(CN)_2^-]_n$ oligomer ions are much stronger than the corresponding ground-state aurophilic and argentophilic interactions. The Au−Au bonds are stronger in the ground state and weaker in the first excited state than the corresponding Ag−Ag bonds.

Acknowledgment. Acknowledgment is made to the donors of the Petroleum Research Fund, administered by the American Chemical Society, and the Robert A. Welch Foundation, for the support of this research. We thank the Laboratory for Molecular Simulations and the supercomputing facilities at Texas A&M University for providing the software and computer time for the MP2 calculations. The technical assistance with the MP2 calculations by Lisa M. Thomson is greatly appreciated.

JA011176J

(77) (a) Celestino, K. C.; Ermler, W. C. *J. Chem. Phys.* **1984**, *81*, 1872. (b) Houtermans, F. G. *Helv. Phys. Acta* **1960**, *33*, 933.

(78) (a) Callear, A. B. *Chem. Rev.* **1987**, *87*, 335. (b) Morse, M. D. *Chem. Rev.* **1986**, *86*, 1049.